Study on thermal and strain behaviour in selective laser sintering process

Study on Thermal and Strain Behaviour in Selective Laser Sintering Process

Mohd Sanusi Abdul Aziz[1, a],Tatsuaki Furumoto[2,b],Takashi Ueda[2,c], Satoshi Abe[3,d],Akira Hosokawa[2,e]and Ryutaro Tanaka[2,f]

[1]Graduate School of Natural Science and Technology, Kanazawa University, Kakuma-machi, Kanazawa, Ishikawa 920-1192, Japan

[2]Institute of Science and Engineering, Kanazawa University, Kakuma-machi, Kanazawa, Ishikawa 920-1192, Japan

[3]Panasonic Electric Works Co., Ltd, 1048 Kadoma, Kadoma, Osaka 571-8686, Japan

[a]msanusi@stu.kanazawa-u.ac.jp, [b]furumoto@t.kanazawa-u.ac.jp, [c]ueda@kenroku.kanazawa-u.ac.jp, [d]sabe@panasonic-denko.co.jp, [e]hosokawa@t.kanazawa-u.ac.jp, [f]r-tanaka@t.kanazawa-u.ac.jp

Keywords: layered manufacturing, selective laser sintering, Yb:fibre laser, residual stress, deformation

Abstract. This paper investigates thermal and strain behaviour in the selective laser sintering process with a mixture of SCM, Cu and Ni metal powder. In-process monitoring of strain change and temperature at the base plate is proposed in order to investigate thermal and strain behaviour induced by selective laser sintering. A strain gauge was attached to the bottom surface of the base plate while a thermocouple was inserted at a distance of 2 mm from the top surface of the base plate. Changes in the strain and the base plate temperature were observed using an oscilloscope during the laser sintering process. The results showed that the development of strain within the sintered structure was affected by the processing temperature. Besides that, after the laser sintering process was completed, the strain value increased gradually and became constant as it reached room temperature. This strain value was found to correspond with the test model's deformation. In addition, the effects of laser scanning direction and laser energy density during the process were observed. Measurement of the test model's deformation was also carried out to discover its relationships to strain change and processing temperature. The results showed that the sintered structure produced by laser scanning of a sector along the width induced less residual strain, which resulted in less deformation. In contrast, both residual strain and deformation were found to be higher when the laser scanning was carried out along the length. Furthermore, when a low laser energy density was used, less deformation of the sintered structure could also be obtained.

Introduction

Layered manufacturing is the most efficient technology in producing prototypes, tools and functional end products. Advanced IT technology has encouraged 3D-CAD application in layered manufacturing which is widely used by automobile, consumer products, medical and many other industries [1]. Recently, a newly developed machine that combines laser sintering and machining processes has attracted the attention of many researchers and manufacturers. By employing this technique, even a complicated mould can be manufactured in a shorter time and also requires less production cost [2]. However, due to the rapid heating and cooling during the laser sintering process, the repetition of thermal expansion and shrinkage generate residual stress within the sintered structure which causes deformation and micro crack problems [3].

In this study, thermal and strain behaviour of sintered material produced by an irradiating Yb:fibre laser on a layer of SCM, Cu and Ni metal powder mixture was analyzed. The understanding of the residual stress development process is very important in order to reduce the residual stress within the sintered structure by optimizing the laser conditions. In-process monitoring of strain change and temperature at the base plate was proposed in order to investigate the thermal and strain behaviour during the sintering process. Additionally, different conditions of laser scanning direction and energy density were also applied to understand their temperature and strain relationships. These results were compared to their deformation results which were obtained by using laser displacement sensor [4].

Experimental Procedures

Laser Sintering Process. The sintering process of metal powder is illustrated in Fig. 1. The system consists of a powder table, sintering table, recoater blade and a Yb:fibre laser (IPG Photonic Corp.: YLR-SM). By using CAD, a 3D model was divided into sliced layers where every layer thickness was 50 μm. Before the sintering process started, a sandblasted steel base plate was placed on the forming table. In order to produce a 50 μm thick sintered layer, the powder table was lifted up while the forming table was moved down respectively. Then, the powder from the powder table was deposited on a base plate by the recoater blade. Subsequently, the laser beam was irradiated on the layer of the deposited metallic powder according to the CAD data. After forming a layer of sintered material, these processes were repeated as the laser scanning direction was varied by 90° until a complete model was created. The laser sintering process was performed in a nitrogen atmosphere at room temperature to prevent oxidization.

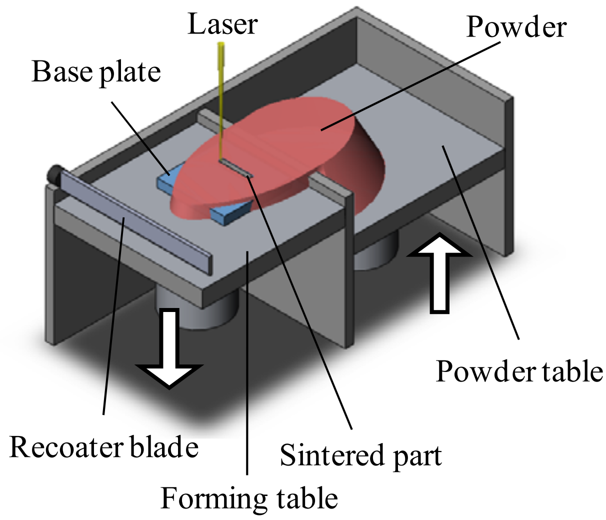

Fig. 1 Schematic illustration of laser sintering process

Test Model. To determine how residual stress develops in sintered material, a beam shaped test model as shown in Fig. 2 was proposed. The specification of the test model is summarized in Table 1. The below part of the test model was the base plate and the upper part was the sintered material. The base plate was sandblasted with #35 of average grain size to improve the wetting property of melted powder [5]. The sintered material was made from a mixture of metallic powder as shown in Fig. 3. The mixture consisted of 70 % chromium molybdenum steel powder, 20 % copper alloy powder and 10 % nickel powder in weight with a mean diameter of 25 μm.

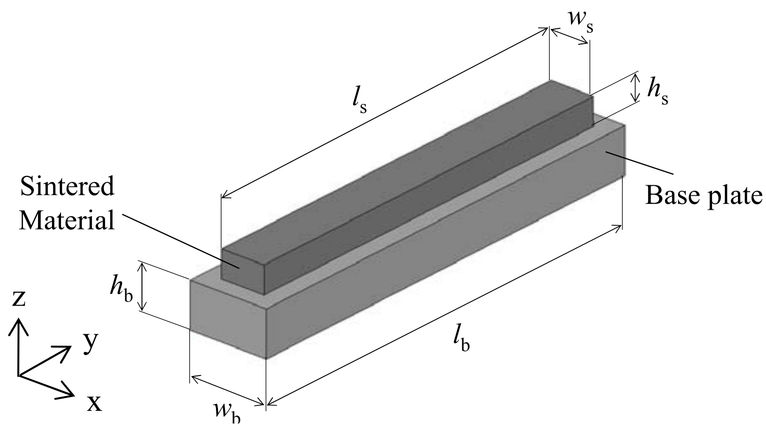

Fig. 2 Schematic illustration of sintered test model

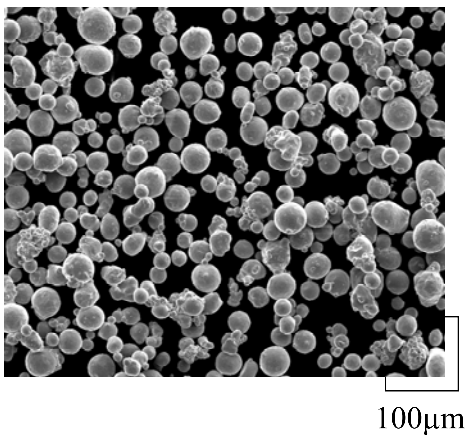

Fig. 3 SEM image of metallic powder

Table 1 Specification of sintered test model

Base plate	Carbon Steel (AISI 1049)
Size $h_b \times l_b \times w_b$	$h_b \times 49 \times 9$ mm
Height h_b	5, 20 mm
Sintering	
Material	SCM, Cu, Ni
Size $h_s \times l_s \times w_s$	$3 \times 45 \times 5$ mm
Layer thickness t	50 μm
Laser beam	
Laser power P	200 W
Scanning speed F	222 - 444 mm/s
Beam diameter ϕ	100 μm

Measurement of Strain and Temperature. A high temperature gradient during the laser sintering process is the main factor causing residual stress development. To understand the behaviour of temperature and strain change during the sintering process, temperature and strain measurement apparatus was introduced as shown in Fig. 4. A type K thermocouple (MISUMI Group Inc.: MSND1.6-50) was inserted into the base plate located at a 2 mm distance from the top surface of the base plate's centre. A strain gauge (Kyowa Electronic Instruments Co., Ltd.: KFG-2-120-C1-11) was attached at the bottom face of the base plate. Both thermocouple and strain gauge were connected to an oscilloscope and their output waves during the sintering process were recorded.

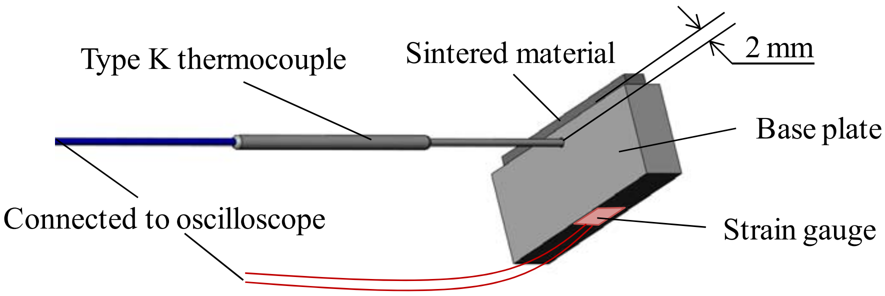

Fig. 4 Schematic illustration of temperature and strain measurement

Laser scanning direction and laser energy density. In this research, different laser scanning direction and laser energy density conditions were used to produce the test model. A schematic illustration from the top view of different scanning directions is shown in Fig. 5. The standard scanning direction was X-Y, which was varied by 90° after forming a layer of sintered material. Laser scanning of a sector along the width and scanning sector along the length were identified as X-X and Y-Y, respectively. On the other hand, different laser energy density conditions used in this research are described in Table 2 and the same scanning direction X-X was used in every condition. Laser energy density is determined by changing the scanning speed according to Eq. 1.

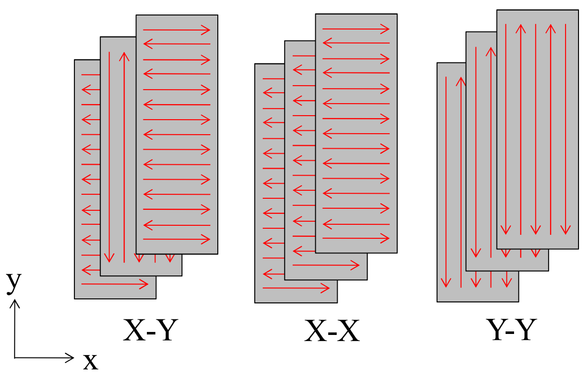

Fig. 5 Laser scan direction

$$E_s = \frac{P}{v\delta} \tag{1}$$

where E_s is laser energy density, P is laser power, v is laser scan speed and δ is laser beam spot diameter [6].

Table 2 Laser energy density conditions

Laser scan condition	Condition description	Laser scan speed
X-X	Conventional laser energy density	1-10th layer : F = 222 – 444 mm/s 11 – 60th layer : F = 444 mm/s
$X\text{-}X_{low}$	Low laser energy density	1-60th layer : F = 444 mm/s
$X\text{-}X_{high}$	High laser energy density	1-60th layer : F = 222 mm/s

Results and discussion

Relationship between temperature and strain. The temperature and strain history of the base plate during the sintering process is shown in Fig. 6. The scan direction used in this sintering process was X-Y for 60 layers. From the magnified image of the temperature and strain history, it was found that during laser irradiation of metallic powder in the X direction, the temperature of the thermocouple rose gradually when nearing the centre of the base plate. At the same time, the strain value of the strain gauge located at the bottom face of the base plate decreased or experienced shrinkage which means that the irradiated layer underwent thermal expansion. Then, as soon as the laser stopped and the new layer of metallic powder was deposited, the strain rose which means that during the cooling process, the melted layer shrank. The thermal expansion and shrinkage processes also occurred during laser irradiation in the Y direction. The last melted layer was expanded during the heating process and shrank during the cooling process and this repetition produced residual stress within the sintered material. The shrinkage was found to exceed the elastic limit (yield strength) of the sintered material which led to permanent deformation.

By observing the overall temperature and strain history, at the early stage of the sintering process, it was noticed that the temperature of the base plate increased gradually while at the same time the strain at the bottom face of the base plate rose to the compressive stress zone. Then, as the sintering process continued, the temperature remained constant around 80 to 120 °C until the sintering process completed. However, in this period the strain increased towards the tensile stress zone. This showed that the shrinkage process was superior to thermal expansion of the sintered layer. After the laser

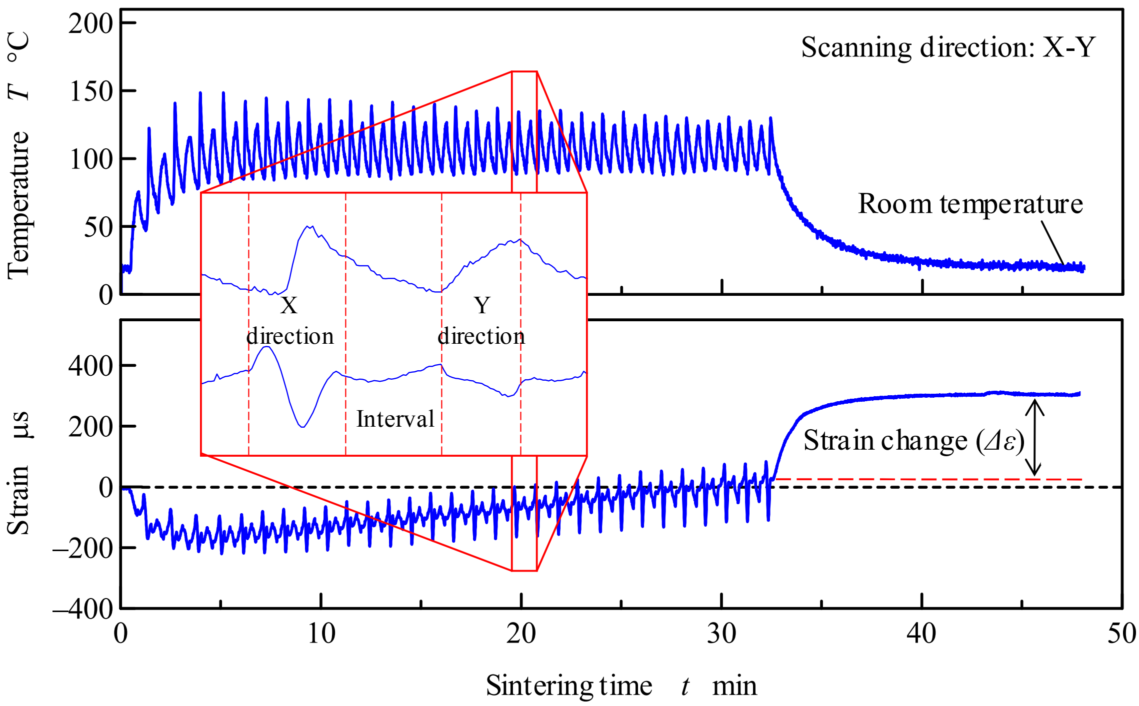

Fig. 6 Temperature and strain history during sintering process

sintering process was completed, the strain value increased gradually and became constant as it reached room temperature. The difference of strain change ($\Delta\varepsilon$) from the finished-point of the sintering process to the point when it reached room temperature was found to correspond with the base plate's deformation after the sintering process completed.

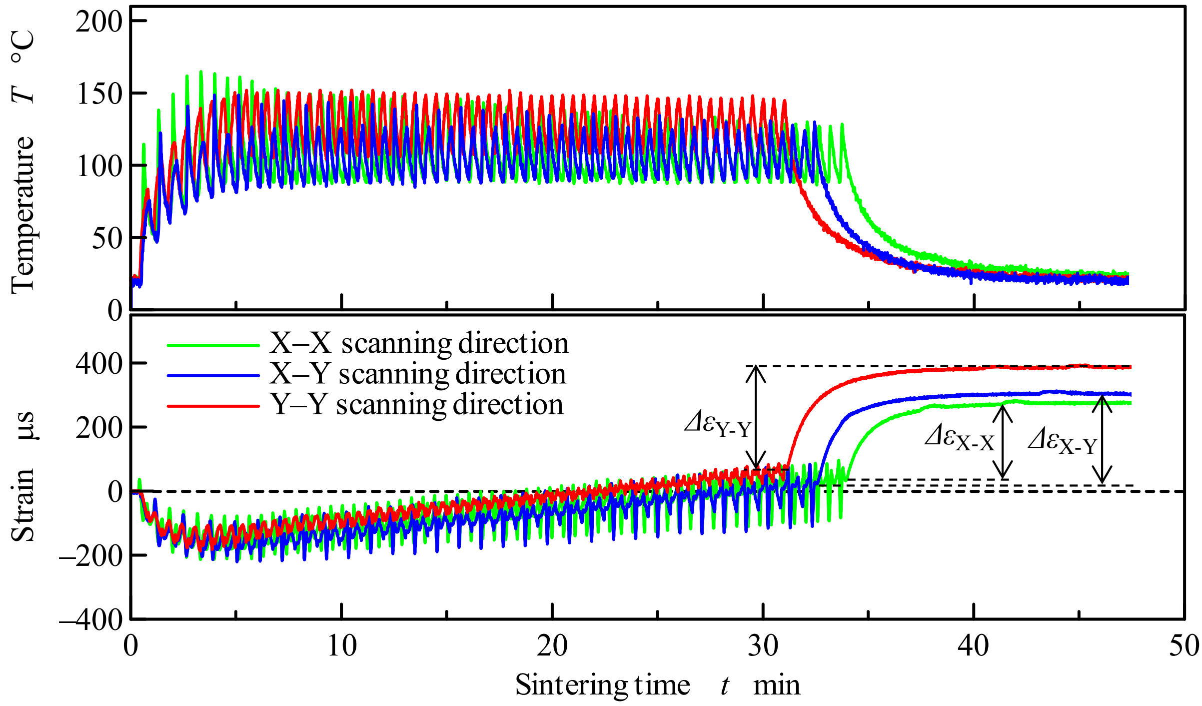

Fig. 7 Temperature and strain history during sintering process

Effects of Scanning Direction. Fig. 7 shows the base plate's temperature and strain history during the sintering process of different laser scan directions. From the temperature history result, by scanning a sector along the length condition (Y-Y), the temperature change was higher compared to the X-Y and X-X conditions. Furthermore, when the sintering process was completed and reached room temperature, the strain change $\Delta\varepsilon_{Y\text{-}Y}$ (310 με) was the highest, followed by $\Delta\varepsilon_{X\text{-}Y}$ (270 με) and $\Delta\varepsilon_{X\text{-}X}$ (250 με). This result corresponds to the deformation result of the scan direction conditions which is shown in Fig. 8. The Y-Y scan direction had the highest deformation of 160 μm. In contrast, the X-X scanning direction condition which had the smallest strain change ($\Delta\varepsilon_{X\text{-}X}$) at the end, resulted in the smallest deformation compared to the Y-Y and X-Y scan directions.

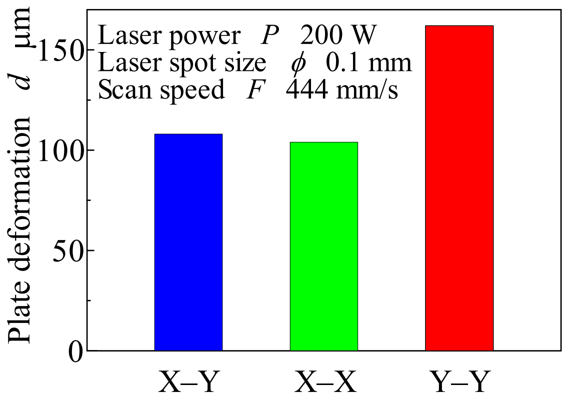

Fig. 8 Model deformation by different laser scan direction

Effects of Laser Energy Density. Fig. 9 shows the base plate's temperature and strain history during the sintering process with different energy density conditions. From the strain history, high energy density condition $X\text{-}X_{high}$ produces the highest strain change $\Delta\varepsilon$ (280 με) after reaching room temperature followed by conventional energy density condition X-X (250 με) and low energy density condition $X\text{-}X_{low}$ (220 με). The high energy density condition produced a high temperature change during the sintering process, which generated a high strain change ($\Delta\varepsilon$) after the sintering process completed. This result also corresponds to the deformation result of those conditions which is shown in Fig. 10. High energy density condition $X\text{-}X_{high}$ resulted in higher deformation within the sintered material compared to the X-X and $X\text{-}X_{low}$ conditions.

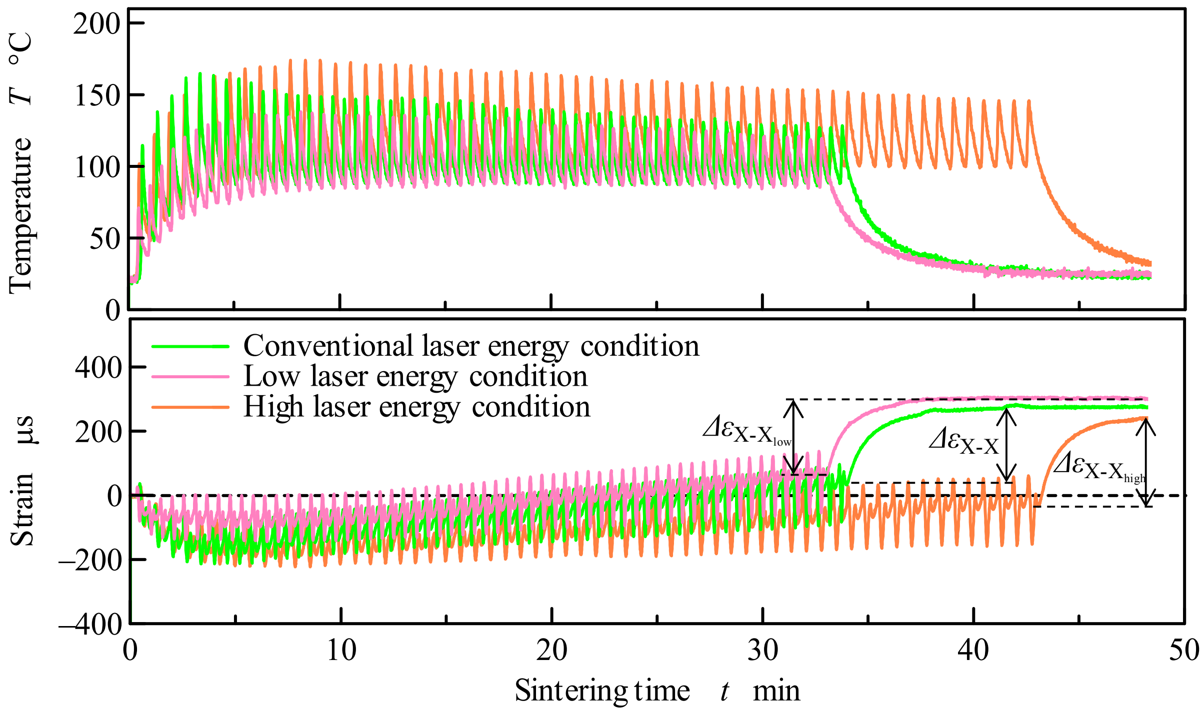

Fig. 9 Temperature and strain history by different laser energy density

Summary

The main results obtained are summarized as follows:

(1) Development of strain, which results in residual stress within the sintered structure, was affected by the repetition of a thermal expansion and shrinkage mechanism.
(2) Laser scanning of a sector along the width induced less residual strain, leading to less deformation.
(3) Low laser energy density used in the sintering process produced less deformation.

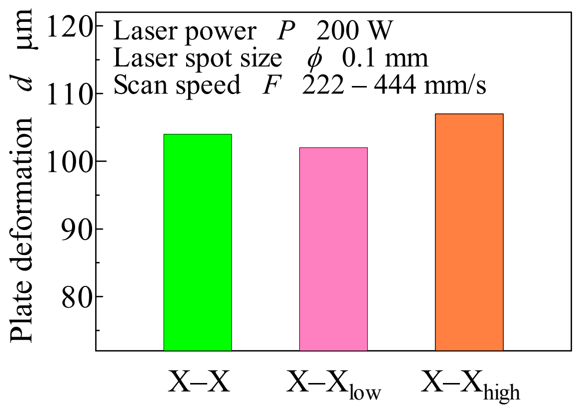

Fig. 10 Model deformation by different laser energy density

References

[1] T. Wohlers, Wohlers Report 2000, Wohlers Associates, Colorado, 2000.
[2] S. Abe, Y. Higashi, I. Fuwa, N. Yoshida and T. Yoneyama, Milling-Combined Laser Metal Sintering System and Production of Injection Molds with Sophisticated Functions, In: Proc. of 11th International Conference on Precis. Eng., Tokyo, Japan (2006) 285–299.
[3] M. Shiomi, K. Osakada, K. Nakamura, T. Yamashita and F. Abe, Residual stress within metallic model made by selective laser melting process, Annals of the CIRP, Vol. 53, No. 1 (1991) 195.
[4] T. Furumoto, T. Ueda, M.S.A. Aziz, A. Hosokawa and R. Tanaka, Study on Reduction of Residual Stress Induced in Rapid Tooling Process, Influence of Heating Conditions on Residual Stress, Key Engineering Materials, 447-448 (2010) 785
[5] T. Furumoto, T. Ueda, A. Hosokawa, Y. Abdullah and S. Abe, Study on sintering characteristics of the mixed metal powder with Yb fiber laser, Evaluation of the adhesion force of the sintered material on the different surface plate, J. Jpn. Soc. Precis. Eng., Vol.74, No.8 (2008) 836.
[6] L. Lü, J.Y.H. Fuh, Y.S. Wong, Laser-induced Materials and Processes for Rapid Prototyping, Kluwer Academic Publishers 2001.